

# Thermal Stability of Foils Made of Graphene-Oxide and Grapheme -Oxide with Fullerene and their Composites with Methyl Car Boxyl Cellulose and with Beta 1, 3/1, 6 -D-Glucan

Zemanová Eva<sup>1</sup> and Klouda Karel<sup>2</sup>

<sup>1</sup> VAB-Technical University of Ostrava

Received: 9 December 2013 Accepted: 31 December 2013 Published: 15 January 2014

---

## Abstract

This contribution contains data on thermal stability of certain materials whose initial precursor is graphite. Graphite was oxidized separately and in a mixture with fullerene C<sub>60</sub>. The prepared oxides were processed with vacuum filtration to produce foils and their morphology and thermal stability was described. The graphene oxides reacted with nano-cellulose and β-glucan to produce composites. The prepared composites in the form of foils were tested for thermal stability and further analyzed e.g. by FT-IR, SEM, etc.

---

**Index terms**— grapheme oxide, fullerene - c<sub>60</sub> Intercalate, composite, nano-cellulose, β-glucan.

## 1 Introduction

Graphite is an allotropic modification of carbon with sp<sup>2</sup> bonds and made up of layers of mutually interconnected hexagonal rings. The layers are arranged in parallel planes 335 pm apart. Carbon atoms in the adjoining layers are not chemically bonded to each other and they are attached by weak van der Waals forces that make it possible for various atoms or molecules in liquid or gaseous form to get in between the carbon layers. The resulting substances are called intercalation compounds of graphite and their characteristic parameter is the so-called "degree of intercalation", which indicates the number of carbon layers between two layers of an intercalated substance (Klouda, 1985).

Depending on a type of the intercalated substance the graphite plane may be either an acceptor or donor of electrons. Another option is the so-called π-complex created by intercalation of substances of AX<sub>y</sub> type, where A is a metal or non-metal with a high intercalates of graphite with alkali metals have been known since 1930s. They are called intercalates of the first degree with the formula C<sub>8</sub>M (M=K, Rb, Cs), i.e. they are characterized by a stacking sequence of layers of carbon and alkali metal.

Intercalates of graphite with alkali metals or in combination with other metals have been used in a number of applications as catalysts, e.g. for synthesis of ammonia, synthesis of carbohydrates by hydrogenation of carbon oxides, hydrogenation of olefins, they have sorption properties etc. (Klouda, 1985). Substituents can be chemically bonded to graphite under certain conditions by fluorination or oxidization.

Fluorination of graphite with elemental fluorine at 400-600°C produces a covalent compound called fluoro-graphite CF<sub>x</sub>, x=0.25-1.12, depending on reaction conditions of the fluorination (Klouda, 1985). Oxidization of graphite with strong oxidizing agents produces grapheme oxide (GO), which is a precursor for chemical preparation of graphene (Makharza et. al., 2013).

Publications dealing with oxidization of graphite to prepare G-O usually specify a method used as described by specific authors: Hoffmann (HNO<sub>3</sub>, KClO<sub>3</sub>), Staydennauer (HNO<sub>3</sub>, KClO<sub>3</sub>), Tour (P<sub>2</sub>O<sub>5</sub>, KMnO<sub>4</sub>), Hummers (NaNO<sub>3</sub>, KMnO<sub>4</sub>). In all those methods the main chemical agent used is concentrated sulfuric acid (Chang and Pumera, 2013).

GO is a compound made up of a carbon skeleton with main functional groups, such as carboxyl, carbonyl, epoxy and ether group and hydroxy-groups. These functional groups enable chemical reactions of GO (Zang et. al., 2011) to form covalent bonds with other compounds (e.g. esterification, amidation).

Another option is a GO reaction to form noncovalent bonds (Makharza et. al., 2013). The possible types of the bonds are hydrogen bonds, van der Waals forces, H- $\pi$ , cation- $\pi$ , anion- $\pi$ ,  $\pi$ - $\pi$ , electrostatic forces. These non-covalent bonds are employed in preparation of composite polymers, biopolymers (Yoo, B. M. et. al., 2013) and in use of GO adsorption and absorption properties (Kyzas et. al., 2014; Fakhri et al., 2013; engineering, optics (Russo et. al., 2013) and biomedicine (Shen et. al., 2012).

Graphene can be prepared by a chemical method which consists in reduction of oxidized carbon (functional groups) in GO with various reducing agents (hydrazine, metal hydride, hydrogen, hydrogen iodide) or reducing methods, such as reflux in a polar solvent, microwaves irradiation, electrochemical reduction (Dreyer et. al., 2010).

The composition of graphene-oxide and its decomposition by an exothermic reaction indicates a potential fire risk. This shall apply mainly to industrial production, processing and storage of GO-materials. If stored in a solid form GO shall be protected against sources of heat, electric discharges and exposure to high-intensity light. A question which appeared in publications by Krishnan et al. (Krishnan et al., 2012), i.e. whether GO is a fire retarder or a fire hazardous material, has defined the objective of this work in which we want to assess the behavior of GO and GO-C 60 foils and their composites with cellulose and  $\beta$ -glucan when thermally exposed.

**b) Preparation of Graphene-Oxide (GO) and Graphene-Oxide + C 60 (GO-C 60)**  
Graphite was oxidized with a mixture of  $H_2SO_4$ ,  $KMnO_4$  and  $NaNO_3$  according to Hummers and Offerman (Hummers and Offerman, 1958). Graphite, sulfuric acid and sodium nitrate (for experiments I-II also fullerene C 60), were placed into a flask, the mixture was stirred and cooled to  $10^\circ C$ . Potassium permanganate was subsequently added into the reaction mixture through a hopper in small doses. The mixture with the permanganate was slowly heated to  $60^\circ C$  and stirred at that temperature for 3 hours. Then it was left to stand for three days at the laboratory temperature.

The obtained product was filtered off, washed with a big quantity of distilled water until a negative reaction to sulfate anions and dried for three days on a Petri dish at  $50-60^\circ C$  to form foils of GO or GO-C 60. In order to confirm or to refute our theoretical assumptions about the behavior of fullerene in an oxidation mixture we have performed an experiment in which we maintained mutual ratios of carbon to the other reagents as those used in the experiment with graphite (0.7g C 60, 1 g  $NaNO_3$ , 2 g  $KMnO_4$ , 18 ml  $H_2SO_4$ ). Also the reaction times and subsequent treatment were equivalent. After vacuum filtration we did not obtain foils but after the drying we obtained a black loose powder (hereinafter C 60oxi). The powder was investigated with FT-IR, TGA, DSC analysis and the results were compared with analyses of the initial fullerene.

**d) Reaction of GO and GO-C 60 Foils with Cellulose in Acid Environment**  
GO (0.3 g) and GO-C 60 (0.3 g) foils were placed into Erlenmeyer flasks and 10 ml of distilled water was added. The foil changed into a suspension after 3 days of irregular stirring and short-term ultrasonication. Subsequently, cellulose was added into the flasks (0.65 g) and 8 ml  $H_2SO_4$  (96%). The reaction was exothermic. The mixture was ultrasonicated in a water bath at  $40^\circ C$ . Then the flask content was poured into 50 ml of distilled water and neutralized with a solution of sodium hydrogencarbonate ( $NaHCO_3$ ) until a neutral reaction. The product was then vacuum filtered and washed on a filter with ca. 40 ml of distilled water, dried at  $50^\circ C$  on a Petri dish on which it formed foils.

**e) Reaction of GO with  $\beta$ -Glucan**  
Graphene oxide (prepared according to Hummers, 1958) ii. Employed methods: Ultrasonication with PS4000A, power output 500W, thermostat  $0-77^\circ C$ , frequency 35 kHz. ATR analysis by means of FTIR spectrometry was performed using the spectrometer Bruker Alpha/FT-IR, ART crystal (identified as Platinum Diamond 1 Ref1), software OPUS 6.5, source IR SiC Globar. The number of spectrum scans was 24, resolution  $4\text{ cm}^{-1}$ , spectrum range  $375-4000\text{ cm}^{-1}$ .

Thermal analyses TGA and DSC of the prepared samples were performed on STA 1500, Instrument Specialists Incorporated-THASS, analytical scale SUMMIT, SI 234-4, at flow rate 20 ml/min., heating rate  $10^\circ C/min.$ , ceramic crucible, diameter 5 mm and height 8 mm, degradation medium: air.

Morphology of the samples was determined with SEM Phenom FEI and SEM FEI Quanta 650 FEG (USA) into Erlenmeyer flasks with 25 ml of distilled water. No suspension was formed after 48 hours and it was necessary to perform repeated ultrasonication 5x 2 minutes to prepare the suspension.  $\beta$ -glucan (0.45 g) was added into the suspensions and in one of the flasks also 0.7 ml of concentrated  $H_2SO_4$  (an exothermic process occurred after the acid was added).

i. Visualization of the flask content

? without  $H_2SO_4$  gel (product I)

? with  $H_2SO_4$  suspension (product II) Subsequently, Erlenmeyer flasks were placed into a water bath ( $40^\circ C$ ) and ultrasonicated 3 times for 2 minutes. Then they were left to stand for 15 days at the laboratory temperature. The flask with the product I (GO- $\beta$ G) was vacuum filtered and the resulting black foil was dried at  $50-55^\circ C$ . The flask with the product II (GO- $\beta$ G, H+) was poured into a 300 ml flask, diluted with 200 ml of distilled  $H_2O$  and subsequently 12 times decanted top H 6.5. The flask contained a brown spongy coagulate in 1/3 of the flask volume. A part of the coagulate was vacuum filtered and it formed a brown foil which was dried at  $50-55^\circ C$ .

---

## 2 II.

## 3 Results

### 4 a) Oxidation of Graphite and Mixture of Graphite-C 60

The foil obtained by vacuum filtration from the product of oxidation of graphite alone and the product of joint oxidation with C 60 had clearly different morphologies (see Fig. ??). GO-C 60 foils looked more compact than GO foils. When inspecting the morphology with electron microcopy the GO-C 60 foil has a rougher surface (see Fig. ??). For GO-C 60 foils we also determined its texture. The specific surface of the foil samples GO-C 60 was and the volume of adsorbed monomolecular layer was 5.03 ml/g. The volume of meso pores or macro pores was 0.286 ml/g in comparison with the volume of micro pores which was 0.001 ml/g. The volume representation of meso pores was ca. 286 times higher than that of micro pores. The sample had a mesoporous character with some representation of macro pores. The sample contained very little micro pores (see the volume representation -only 0.001 clogged. The mesopores included the following fractions: 1.5-3 nm (ca. 38%), 3-5 nm (ca. 13%) and 5-10 nm (ca. 5%) and 10-50 nm (ca. 8%). As for macro pores, the sample contained only one fraction, while ca. 24% of the specific surface was formed by macro pores with the diameter 50-200 nm. The measured parameters are shown in Table ?? Subsequently, the foils were examined with X-ray analysis (Fig. 3), FT-IR, TGA and DSC analyses. The X-ray analysis has proved a negligible difference in expansion of the space between the layers, see Fig. When preparing GO by oxidation methods FT-IR is usually indicated as a method for identification of the basic functional groups. In most cases the authors indicate vibration ranges for the given groups: 3000 -3700 cm<sup>-1</sup> ? (-COOH, -OH, H<sub>2</sub>O) 1850 -1750 cm<sup>-1</sup> ? (-C=O) 1650 -1750 cm<sup>-1</sup> ? (carboxy COOH) 1500 -1600 cm<sup>-1</sup> ? (sp<sup>2</sup> C=C) 1280 -1320 cm<sup>-1</sup> ? (epoxides C-O-C) At the same time, ranges that follow may contain the following vibrations: 1280 -1500 cm<sup>-1</sup> : ethers, epoxides, ketones, peroxides, benzoquinone 1100 -1280 cm<sup>-1</sup> : peroxides, ethers, ketones, lactones, anhydrides, epoxides, benzoquinones 900 -1100 cm<sup>-1</sup> : lactones, peroxides, hydroxyls, 1, 3 dioxane, anhydrides, epoxides, carboxylic -OH bond vibration at 3420 cm<sup>-1</sup> , C=O bond vibration at 1720 -1740 cm<sup>-1</sup> .

The mutual comparison of spectrums we obtained for GO and GO-C 60 is shown in Fig. ?? The difference between the GO and GO-C 60 spectrums is in the ratio of the mutual adsorbances for the vibrations: GO 1390 1274 1228 cm<sup>-1</sup> GO-C 60 1378 1278 1228 cm<sup>-1</sup> In the spectrum range 700 -450 cm<sup>-1</sup> the adsorbance of GO has a medium value while for GO-C 60 it is high; in general, GO-C 60 demonstrates higher adsorbances throughout the entire spectrum range. c) Thermal Tests of GO and GO-C 60 foils Two prominent peaks were detected for samples of GO and GO-C 60 foil on the DSC curve (Fig. ??) which corresponded to exothermic processes. The first exothermic process was accompanied by a substantial drop of weight: for GO by 43.6% and for GO-C 60 it was even higher -51.1% (see Tab. 2).

In the case of GO the first exothermic process occurred at 190.9°C with the maximum at 225°C and thermal effect of 508.4 kJ/kg; in the case of GO-C 60 the process started earlier, at 182.6°C with the maximum at 205°C and the thermal effect was lower than for GO. The values of thermal effects in the individual temperature intervals are provided in Tab. 3. The second exothermic effect in the case of GO has its maximum at 450°C, while for GO-C 60 it was already at 390°C and the detailed shape of the curve was different (compare Figures 5 and 6). For GO-C 60 the weight loss during the second exothermic effect was lower than during the exothermic effect in the case of GO, which means a situation different from the first effect.

The weight losses until the first exothermic process are essentially the same for both the foils (ca. 20%) with mild endothermic effects, with a higher thermal effect for GO (anticipated dehydration). Also the overall thermal effect of decomposition is higher for GO-C 60 foil by ca. 30% (see Tab. 3). When performing the experiments we had some expectations about the course and results of their action. The functional groups expected on GO were the following: carboxyl, carbonyl, epoxide, hydroxyl and partly also lactone or sulfonic group. Fullerene C<sub>60</sub> was expected to have the following groups on its molecule: -SO<sub>3</sub>H, -OH, -NO<sub>2</sub>, -ONO<sub>2</sub>, epoxide group. Covalent bonds may form between those groups (esterification, dehydration, addition), as well as noncovalent ones -hydrogen bonds, π-π interaction, van der Waals forces. Also intercalation of a fullerene molecule may occur in the graphene-oxide space. Even breakage of a fullerene molecule in the conditions of oxidation cannot be excluded. One quoted work (Trzaskowski et al., 2013) deals with energy options of a combination of graphene with C 60 on the condition that graphene surface is either defect-free or with defects. Chemical attachment of C 60 on a monolayer of graphene is not possible for energy reasons. However, in presence of various defects on the graphene C-layer, such as e.g. formation of 4- and 5-atomic rings, Stone-Wales defect and other types of defects (e.g. flower defect, octa-penta-, heptadisrupted cyclic formations) may provide space or reactive points for potential bonds with fullerene C 60 .

One of the defects mentioned for the graphene structure is the so-called "adatom" - an adsorbed atom. It is a defect in which e.g. transition metal is adsorbed on the C lattice. Adsorption of transition metals changes physicochemical properties and biocompatibility of graphene or GO (Faye, 2012; Neto, 2009). We have identified a similar defect in the prepared GO: it was e.g. an atom of Fe identified by EDAX in the GO structure (Fig. 7). We performed the so-called blank test to get some notion of how fullerene behaves in the oxidizing environment to which it is exposed jointly with graphite.

## 5 d) FT-IR Analysis of C 60 -Oxi and Initial C 60

The measured IR spectrum of the initial fullerene C 60 is provided in Fig. ???. The main characteristic vibrations for C 60 (Saeedfar et al., 2013) are 522 cm<sup>-1</sup>, 573 cm<sup>-1</sup>, 1159 cm<sup>-1</sup>, and 1426 cm<sup>-1</sup> and they are also a part of the C 60 -oxi spectrum.

For C 60 -oxi (Fig. ??) we have identified an additional weak vibration in the absorption interval 1556-1644 cm<sup>-1</sup> (probably C=C, C=O), 1000-1100 cm<sup>-1</sup> (probably C-O-C epoxy, alkoxy, C-CO-C) and a medium vibration at 702 cm<sup>-1</sup> (probably a substituted aromatic ring). Based on characteristic vibrations of functional groups we can probably exclude presence of the following functional groups on the C 60 -oxi molecule: -OH, -COOH, -COOR, -SO<sub>3</sub>H, -NO<sub>x</sub>. In the measured temperature range, as indicated by the TGA and DSC curves (Fig. ??0-11) up to ca. 420°C, there were no thermal effects on either of the tested samples and the weight loss of both the samples was comparable in units of percents (6.1% for C 60 and 8.6% for C 60 -oxi). In the temperature range of 420-600°C both the samples underwent exothermic reactions, however the thermal effects were very different. The thermal effect of C 60 -oxi was 20 times higher than that of the initial C 60 (1947 kJ/kg for C 60 -oxi and 180 kJ/kg for C 60). The weight loss of C 60 -oxi (56.7%) was twice bigger than that of C 60 (28.8%). The resistance of C 60 -oxi against thermal exposure was partly disrupted. We anticipate partial oxidation of the C-skeleton (IR-spectrum Fig. ??) and thus disruption of its consistency (electron balance) which means that defects can appear in the carbon structure when the material is heated -e.g. the Stone-Wales defect (Kabir et al., 2011).

## 6 Global Journal of Researches in

## 7 Global Journal of Researches in Engineering

We have identified a similar reduction of resistance of the fullerene carbon skeleton in its bromoderivative. After the end of the microdisruption of C-Br bond the C 60 molecule fully (100%) decomposed at 420-550°C.

We are fully aware of the fact that this so-called "blind test" may not completely correspond to the oxidation process in presence of graphite or graphene oxide in which a carbo-catalytic effect may apply (H<sub>2</sub>SO<sub>4</sub>/HCl), ratio of cellulose and acid, time of hydrolysis and on reaction temperature. Naturally, the result is also influenced by the type of the initial cellulose which can come from hard or soft wood, bamboo, sisal, cotton etc. All those factors influence yield and size of the prepared cellulose nano fibers (Ioelovich, 2012; Li and Ragsdale, 2011). The prepared nano crystalline cellulose can be chemically modified, e.g. esterified, carboxylated, oxidized (Peng et al., 2011). It may be also used as a composite in polymers or as a matrix for metal nano particles.

In our case we performed hydrolysis of methyl carboxyl cellulose in presence of suspensions of GO and GO-C 60. We assumed that mutual interconnection may occur by a chemical reaction (e.g. esterification, interconnection with C-O-C bond etc.) or physical chemical bond (e.g. hydrogen bonds). The foils prepared by vacuum filtration of the reaction product were subject to microscopic surface analysis, FT-IR, TGA and DSC analysis.

Morphology of the surfaces as shown by microscopic analysis (see Fig. 12) was different and it suggested a potential method of interconnection between GO / GO-C 60 and nanocellulose. The detailed morphology (electron microscope) of the prepared composite foils is shown in Fig. 13. We assume that in the first case the cellulose hydrolysis was only partial and whiskers of nano cellulose generated after the hydrolysis were of bigger size. At the same time, there was no reaction of C=O groups, unlike in the case of GO, where IR analysis of the product of reaction with cellulose identified no vibration at 1722 cm<sup>-1</sup>, which was present in the spectrum of the original GO. The other vibrations characterizing the groups C-O, C=C, C-O and C-O-C shifted their frequencies and also the mutual absorption ratios were different (Fig. 15).

The same applies in respect to the initial GO, GO-C 60 and cellulose (compare with the spectrums in Fig. ??). For the new products in both cases the IR spectrums did not contain the peaks at 1278 cm<sup>-1</sup> (1274 cm<sup>-1</sup>) and 1228 cm<sup>-1</sup> which in the original spectrums GO-C 60 and GO had the assigned vibrations of epoxy groups.

Similar results, i.e. demonstration of deoxidizing (reduction) process, were described for the mutual reaction of GO with heparin. TGA curves of samples (see Fig. 16) of composites can be divided into several sections with different slopes, i.e. different weight loss rates. This division, including corresponding temperature intervals and corresponding weight losses, is shown in Tables 4 and 5, which provide parameters of the detected thermal processes on the DSC curve.

For composite samples the DSC curve showed one peak corresponding to an endothermic process and two peaks corresponding to exothermic processes. The second exothermic process was very substantial in both the samples. For the GO-C 60 -cellulose sample the exothermic process started at 319.8°C and the peak area on the DSC curve was 3379.2 kJ/kg. Equally significant exothermic process in the GO-cellulose sample started at 341.5°C and the peak area on the DSC curve was 5261. The comparison of thermal stabilities of the prepared GO and GO-C60 composites with cellulose indicates that the foil prepared from GO is thermally more stable but its decomposition releases more thermal energy.

A principal difference can be found when we compare thermal stability (weight loss) of the initial foils of GO and GO-C 60 and thermal stability of their composites with cellulose. The weight loss in the temperature interval 25-220°C was 63% for GO foil and 72% for GO-C 60 foils. For the composites the weight loss was 32% and 22% respectively, which means a major difference. A completely different is the thermal decomposition of the initial cellulose. The decomposition in the temperature interval 25-150°C is accompanied by an endothermic

225 process with the thermal effect 3053.7 kJ/kg and the weight loss of the sample is 64%. i) GO Reaction with  
226  $\beta$ -1,3-1,6-D-Glucan Glucans rank among homopolysaccharides, they have a long chain with only one structural  
227 component-glucose (hexose). Glucose in the chain is attached in the positions 1,3 and 1,6. Smaller chains branch  
228 off from the main chain. The structure of glucans is of extraordinary importance inactivation of the immunity  
229 system where branching of the side chains plays a major role.  $\beta$ -D-glucans are indigestible polysaccharides that  
230 occur in nature in sources such as cereal grains, yeasts, fungi, bacteria and algae. Biological effects of beta-glucans  
231 are manifested at several levels. The main role consists in activation of immunity system cells (macrophage) and  
232 they also perform anti-carcinogenic, antimicrobial, antiviral and antiallergic activities. Beta-glucans also have a  
233 radio protective effect-they deactivate free radicals (Chovancová and Turdík, 2005).

234 We performed reaction of beta-glucan with graphene-oxide under ultrasonication conditions with out sulfuric  
235 acid and in acid environment. j) FT-IR Analysis of the Foils (GO- $\beta$ G and GO- $\beta$ GH+)

236 The obtained spectrums of the products are shown in Fig. 17 from left to right: GO- $\beta$ G, GO- $\beta$ GH+ and initial  
237  $\beta$ G. In the last picture d) the three spectrums are compared. The values of the initial GO are: C-O-C 1068 cm<sup>-1</sup>  
238 , 9.79 cm<sup>-1</sup> , -OH 3149-3186 cm<sup>-1</sup> , -C=C-1613 cm<sup>-1</sup> . k) Thermal Stability of the Product (GO- $\beta$ G, GO- $\beta$ GH+)  
239 and Initial  $\beta$ G

## 240 8 Global

241 The measured results in a graphic form are provided in Fig. 18-20 and interpretation of the TGA and DSC  
242 curves is provided in Tables 6-7. The DSC curve of  $\beta$ G features one peak corresponding to an endothermic thermal  
243 process with minimum weight loss and prominent, partly overlapping peaks that correspond to exothermic thermal  
244 processes which start at 257°C and are accompanied by a significant loss of the sample weight.

245 A common characteristic of both the prepared composite products is that their weight loss curves (TGA) can  
246 be approximated with a line -continuous linear reduction of weight, unlike the step weight loss in case of  $\beta$ G  
247 which was up to 70% (see Fig. 18) and in case of GO up to 60% (see Fig. 19). The products differ from each  
248 other by the number of exothermic effect and the shift of the last exothermic effect by 42°C in favor of GO- $\beta$ G  
249 H+.

250 The overall thermal effect in the course of decomposition decreases from the initial  $\beta$ G to the GO- $\beta$ GH+  
251 composite (see Tab.

## 252 9 Conclusion

253 Joint oxidation of graphite and fullerene C<sub>60</sub> in the ratio 2:1 makes it possible to prepare a compound in form  
254 of compact foils but it has a lower thermal stability and its thermal decomposition is accompanied by thermal  
255 effects that are 30% bigger than effects produced by foils without fullerene. A method of attachment between  
256 oxidized graphite and fullerene has not been demonstrated. The prepared foil can also have other chemical and  
257 physicochemical properties thanks to the fullerene molecule (Troshin et al., 2008).

258 Thermal decomposition of composites of GO and GO-C<sub>60</sub> with nano cellulose is accompanied by bigger thermal  
259 effects than the effects produced by the initial GO and GO-C<sub>60</sub> foils. The same applies also for  $\beta$ glucan in respect  
260 to GO. However, the thermal effect of the decomposition is lower than for  $\beta$ -glucan alone.

261 The products we prepared were in the form of foils (membranes), with the exception of the "blank test" of  
262 fullerene oxidation. GO-foils (papers) are prepared by vacuum filtration of GO dispersion. This is the basic  
263 method of its preparation which we have also applied. We are fully aware of the fact that mechanical, electronic,  
264 chemical and biological properties and the related toxicological properties are affected by many factors which may  
265 have influenced our results of thermal stability measurements. The first factor is the method of GO preparation  
266 and thus the ratio of C/O and topology of the C-skeleton (its defects). The composition of the liquid  
267 phase and the concentration (Park et al., 2012) of the filtered suspension influence the foil thickness, as well as  
268 the filtration rate, and if the suspension is ultrasonicated then also its duration, temperature and power of the  
269 device play a role (Liao et al., 2011). Properties of foils are also influenced by some specific treatments, such as  
270 washing of foils with solution of MCl<sub>2</sub> (Ca, Ba, Mg), while the carbon layers are connected in a plane, across  
271 via dialdehyde (Hu et al., 2011), or its impregnation e.g. with Ti, Ag, Cu

<sup>1</sup>© 2014 Global Journals Inc. (US)

<sup>2</sup>Thermal Stability of Foils Made of Graphene-Oxide and Grapheme -Oxide with Fullerene and their Composites with Methyl Cellulose and with Beta 1, 3/1, 6 -D-Glucan



Figure 1: Figure 1 :Figure 2 :

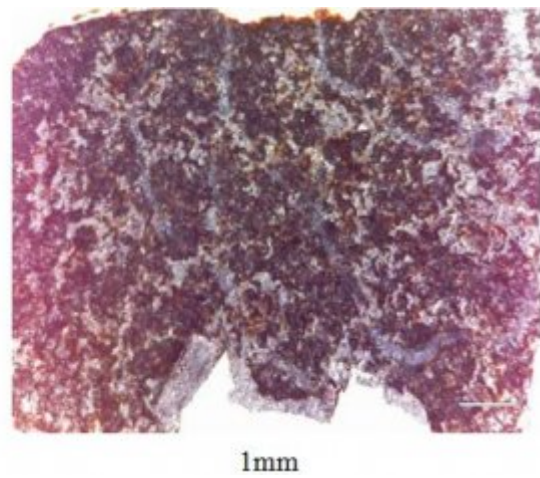
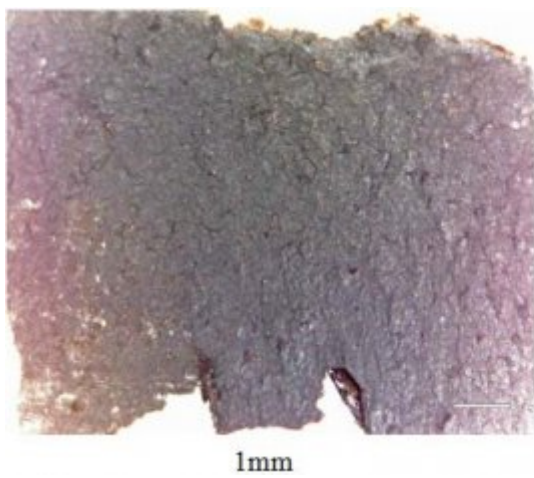


Figure 2:



Figure 3: Figure 3 :

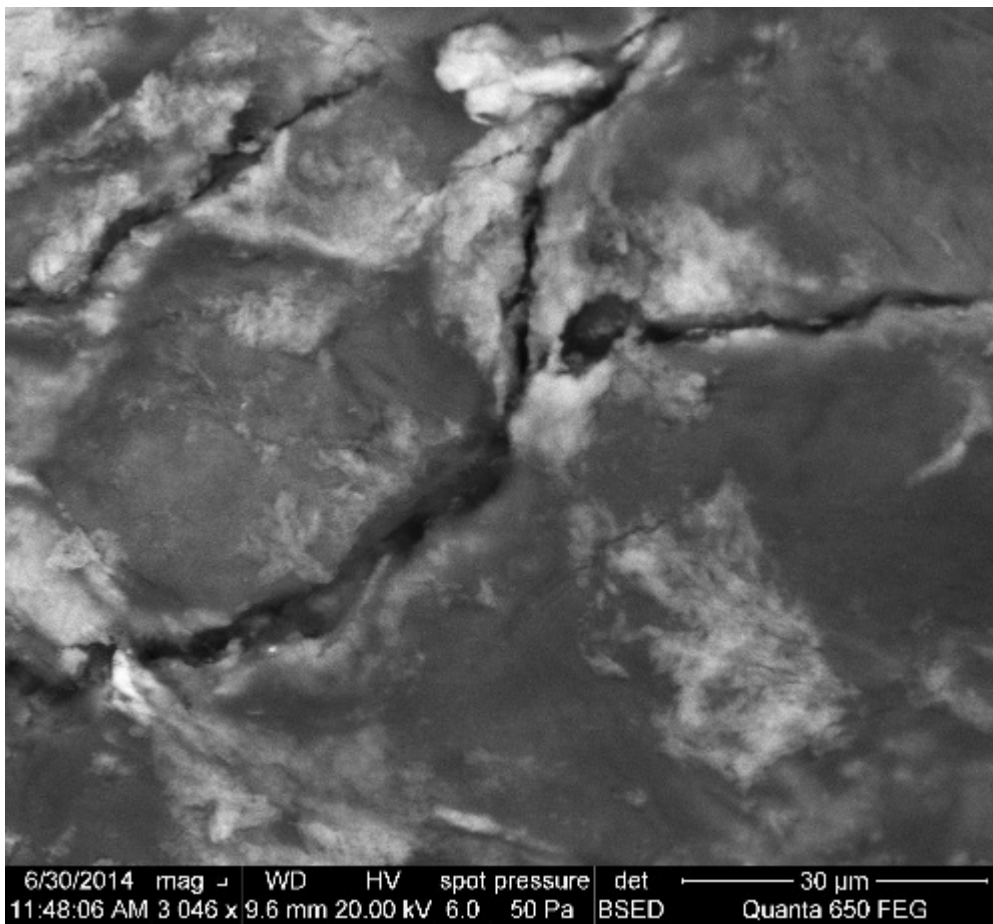


Figure 4:

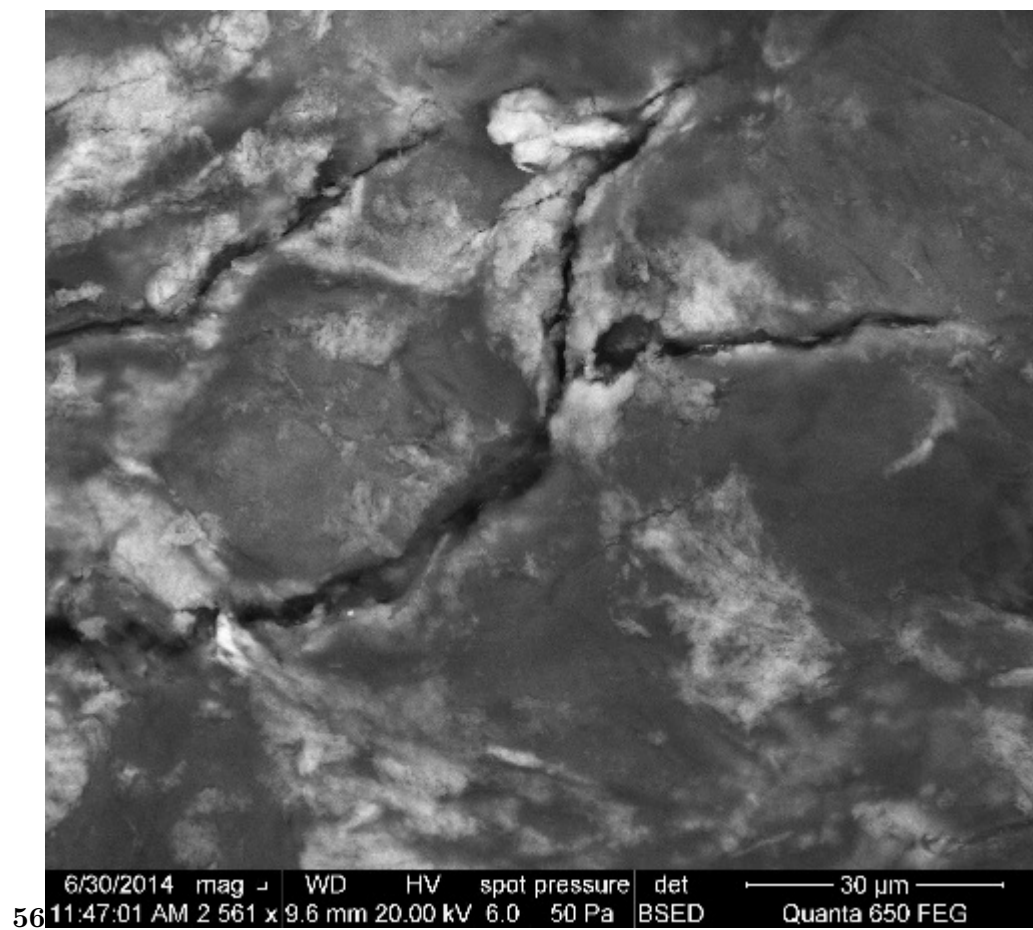


Figure 5: Figure 5 :Figure 6 :

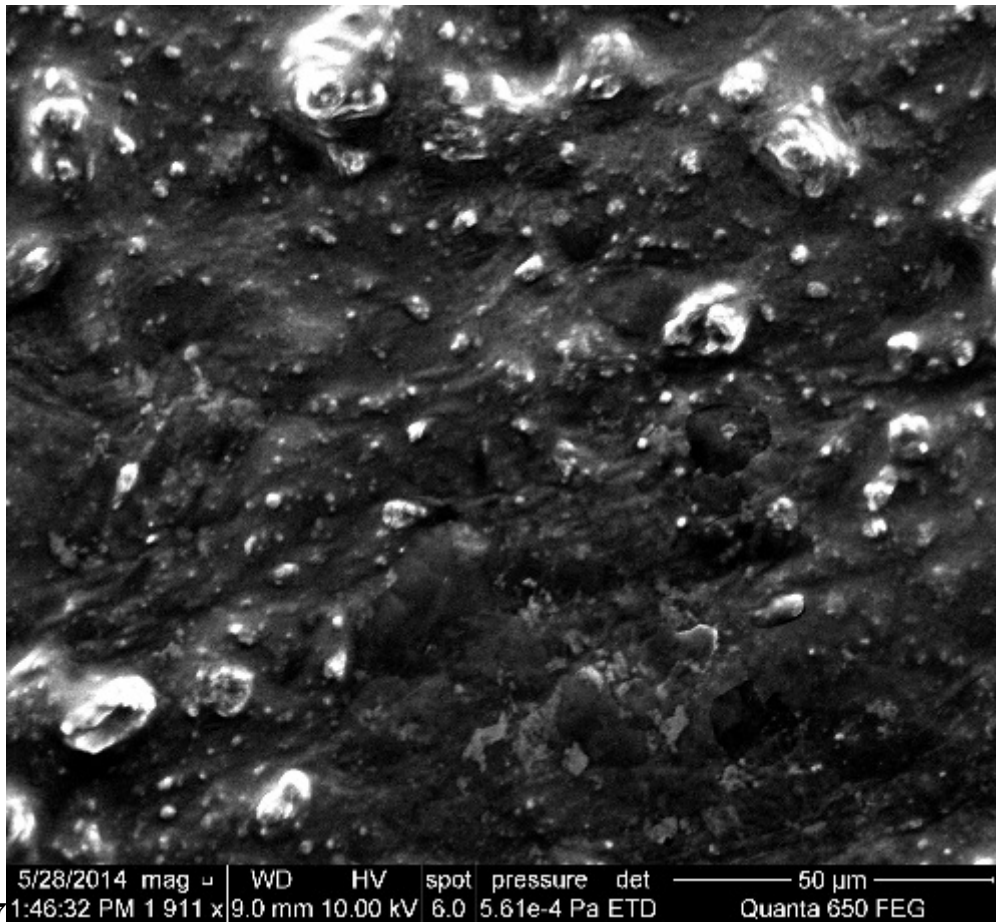


Figure 6: Figure 7 :

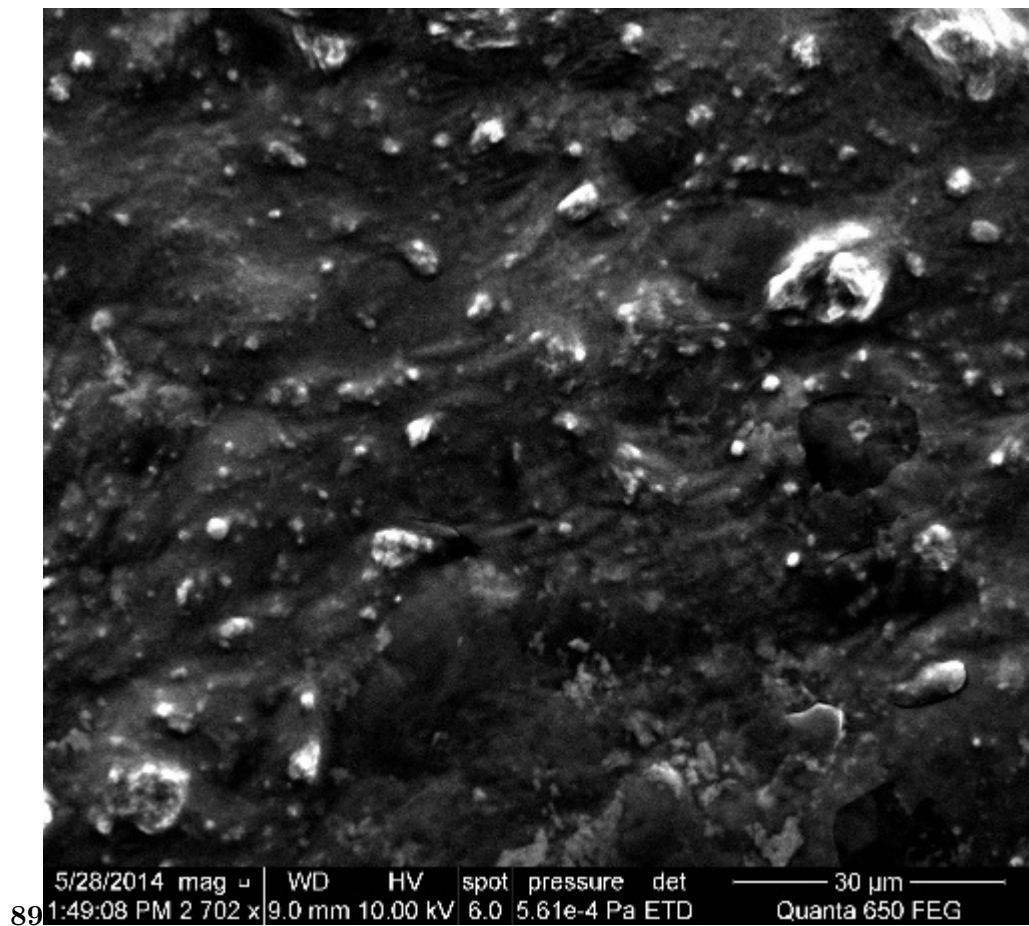
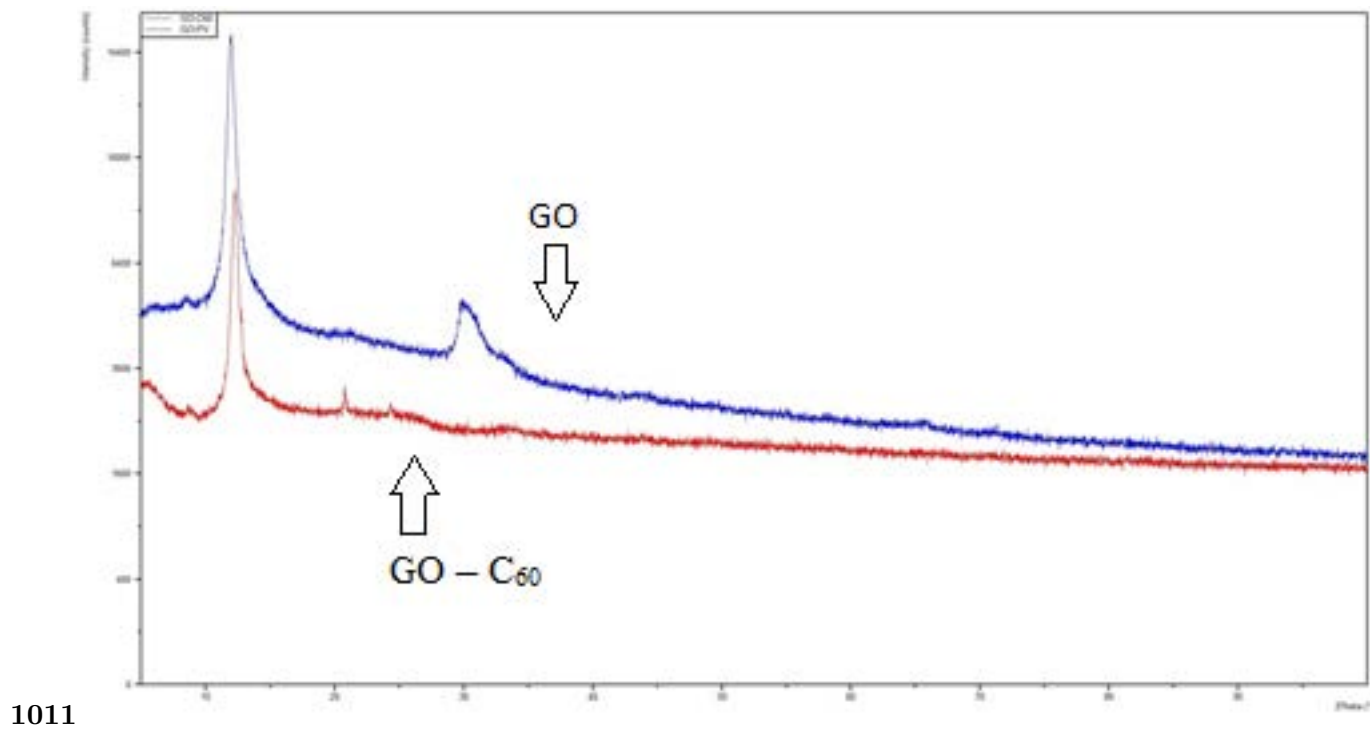


Figure 7: Figure 8 :Figure 9 :



1011

Figure 8: (Figure 10 :Figure 11 :

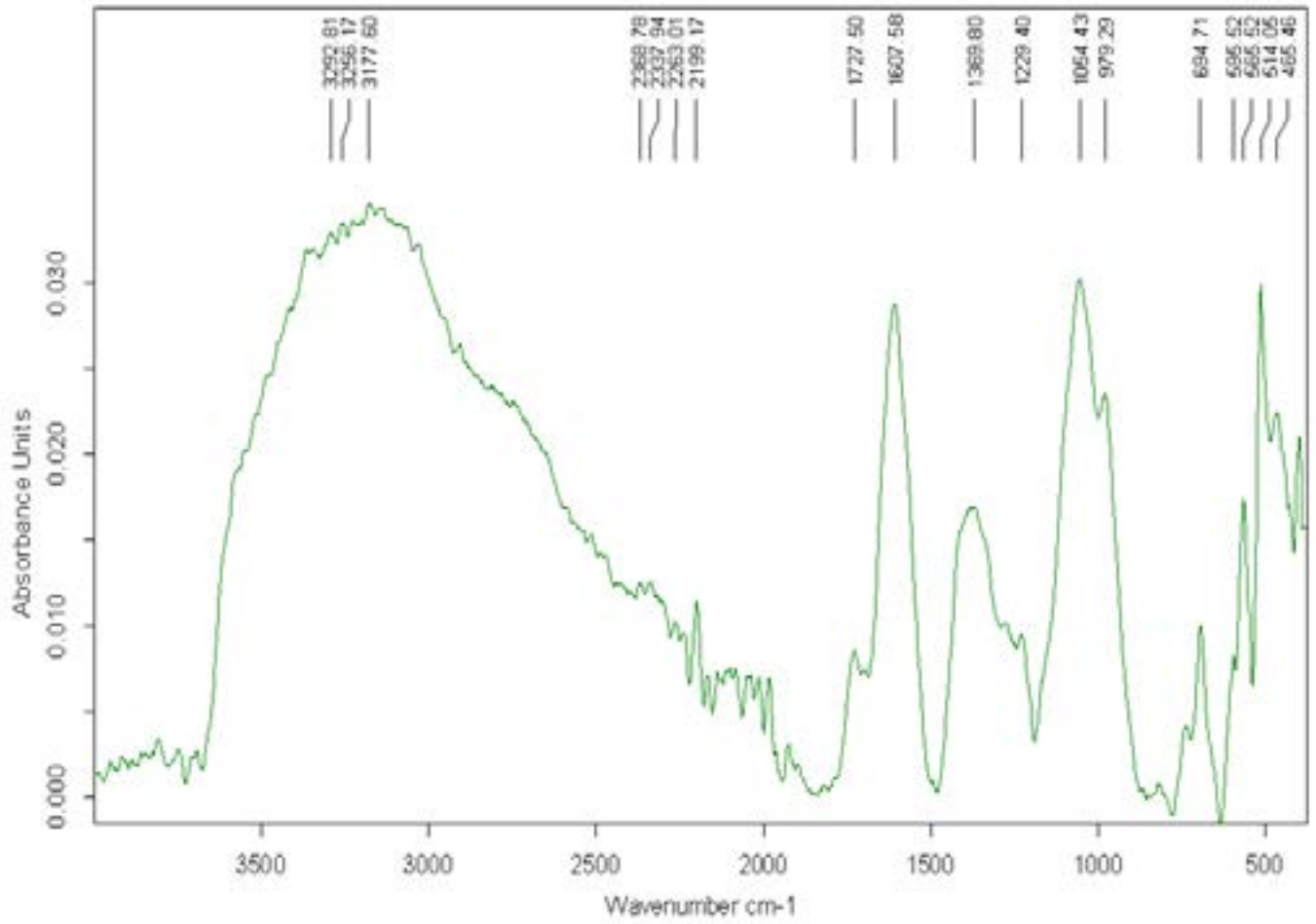
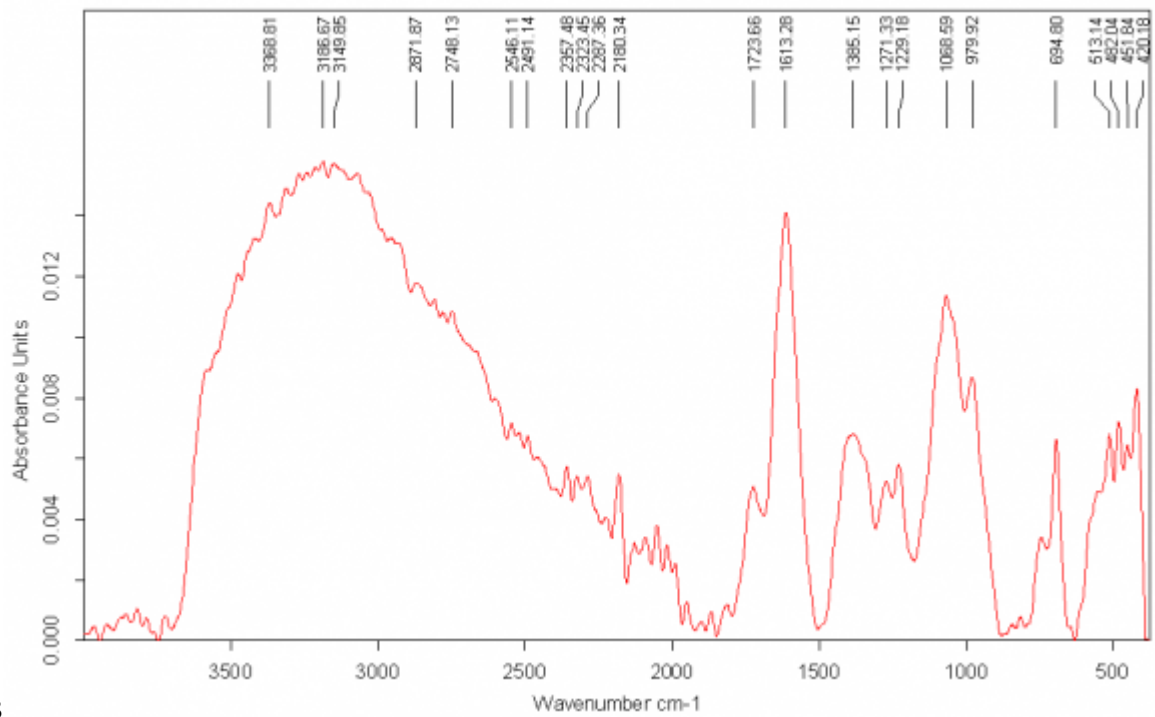


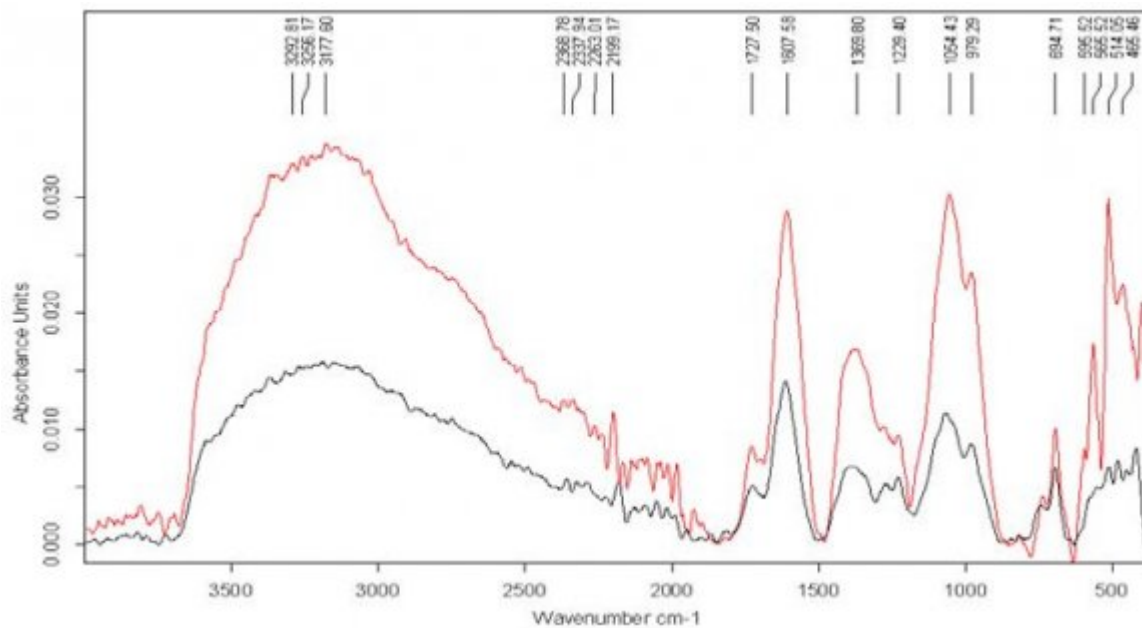
Figure 9: (



1213

Figure 10: Figure 12 :Figure 13 :

## 9 CONCLUSION



15

Figure 11: Figure 15 :

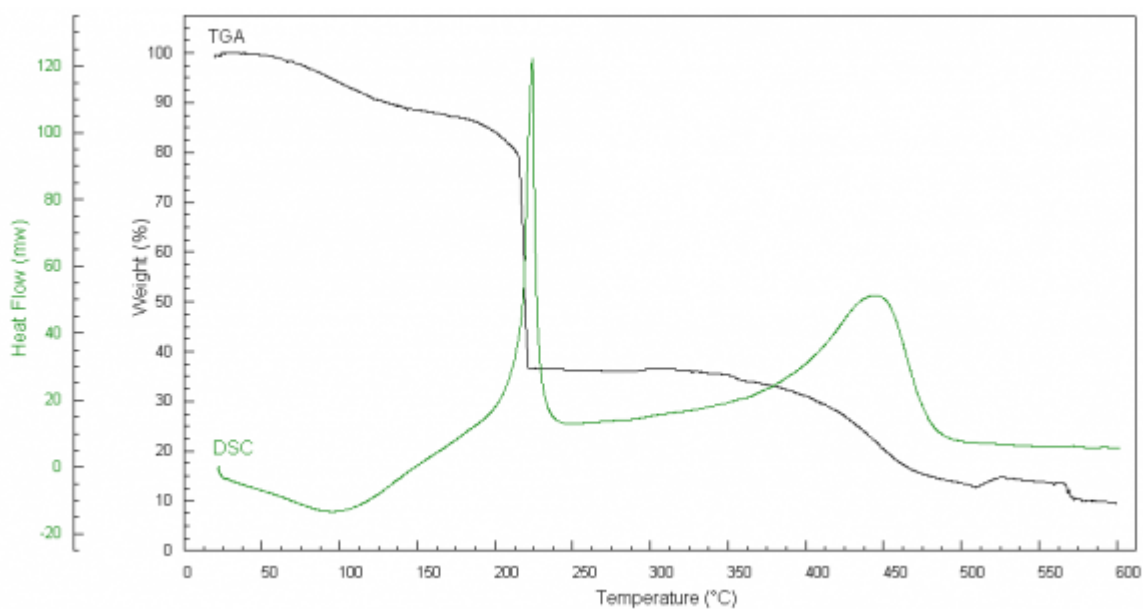
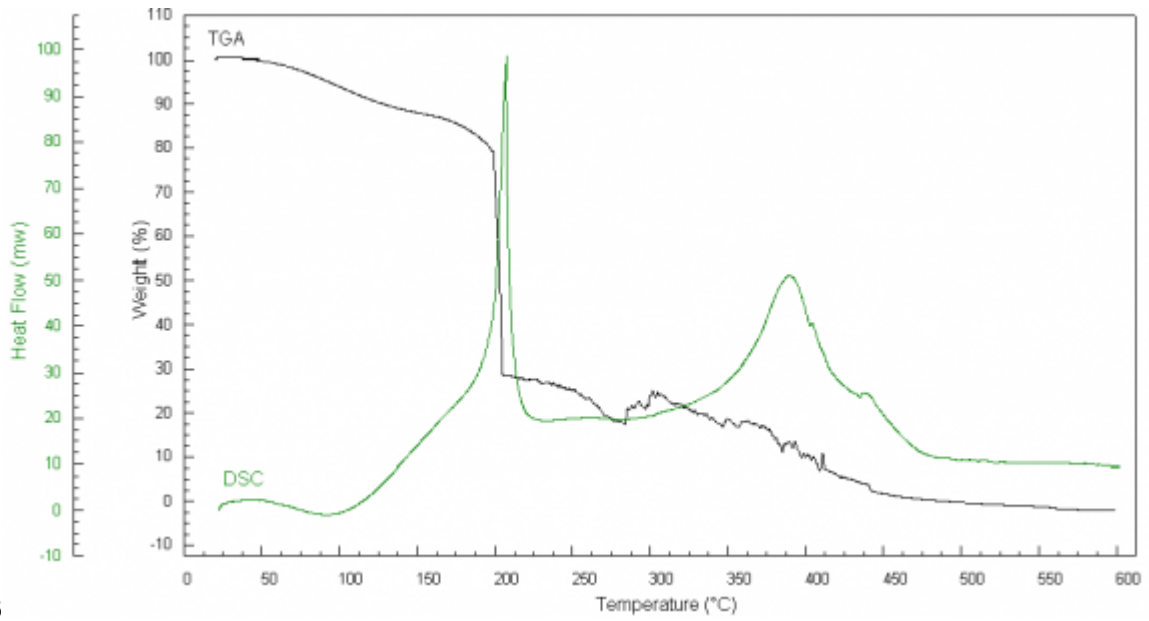


Figure 12:



16

Figure 13: Figure 16 :

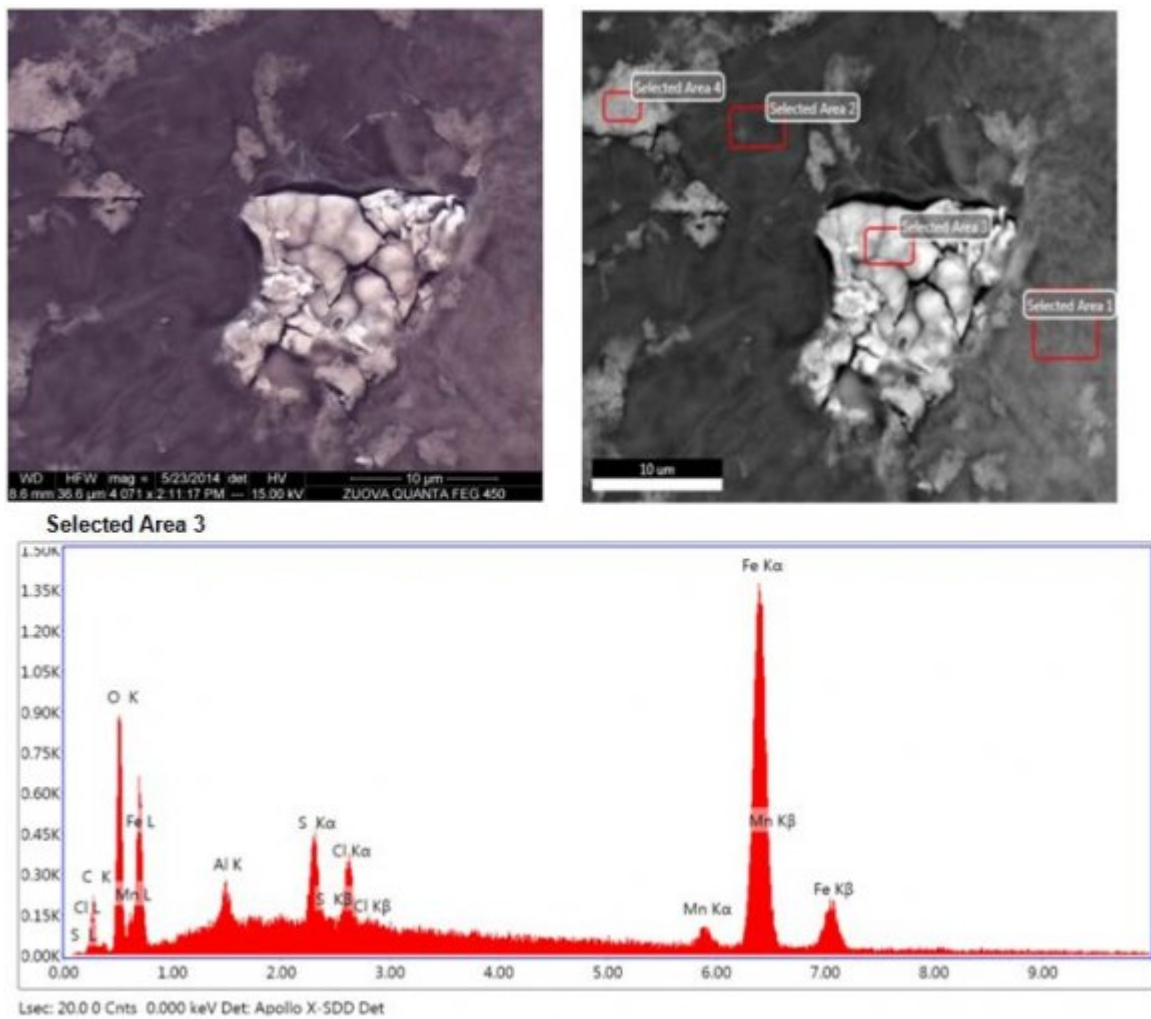
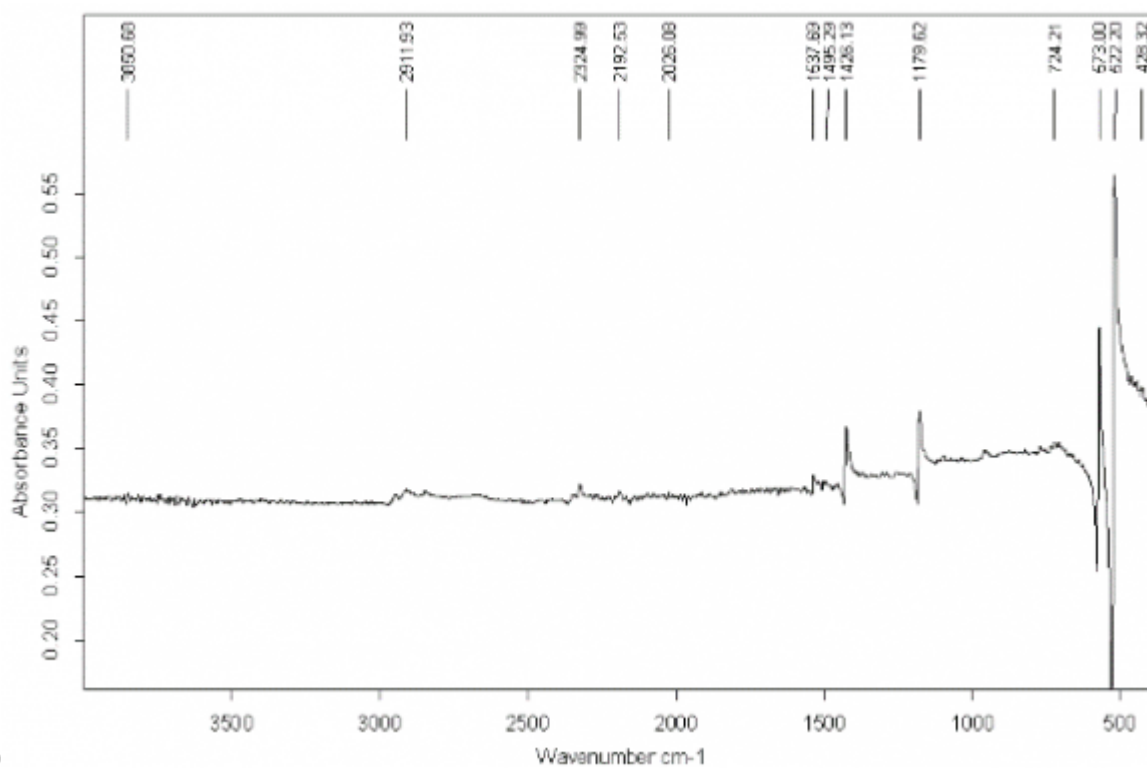


Figure 14:

## 9 CONCLUSION



181920

Figure 15: HFigure 18 :Figure 19 :Figure 20 :

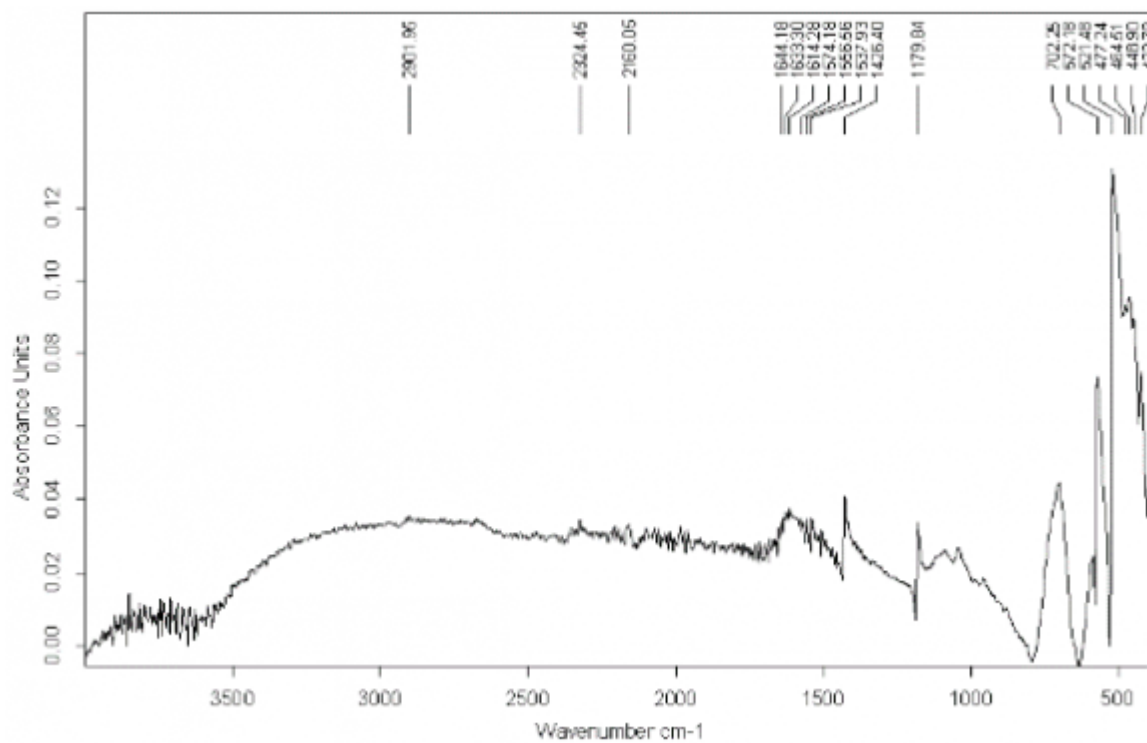


Figure 16:

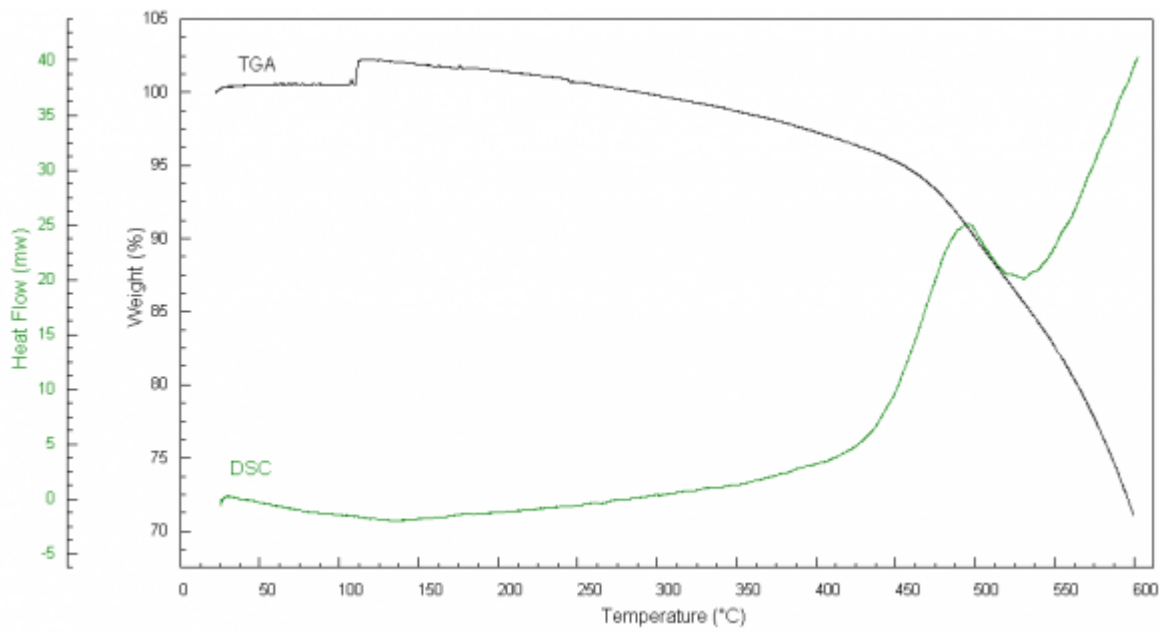


Figure 17:

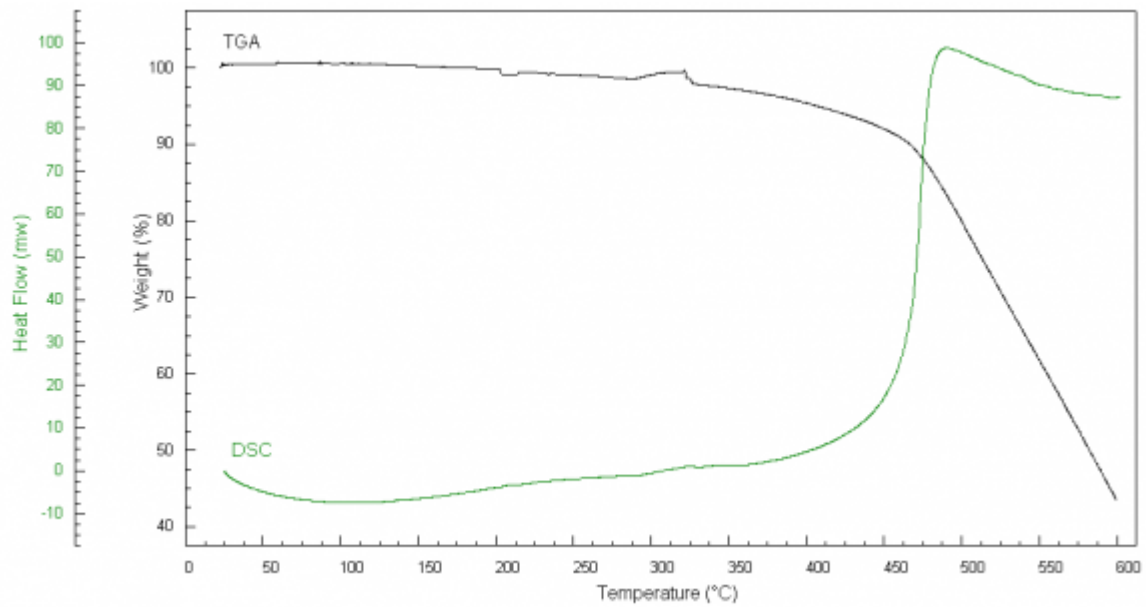


Figure 18:



Figure 19:



Figure 20:

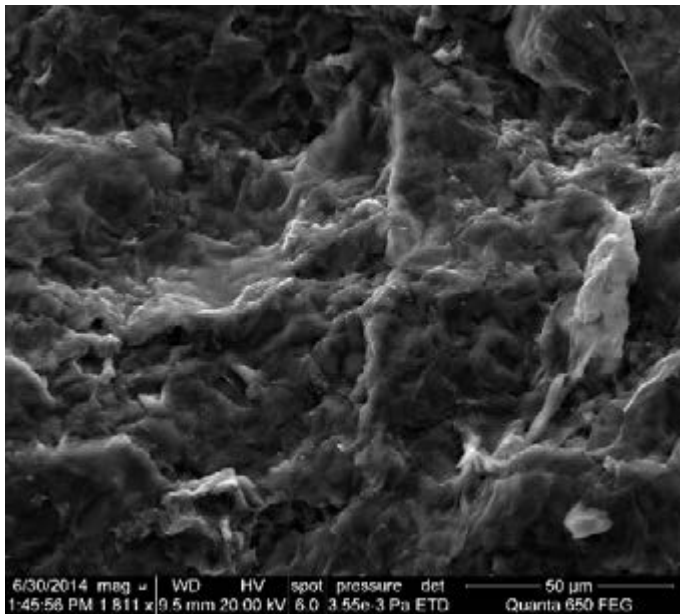


Figure 21:

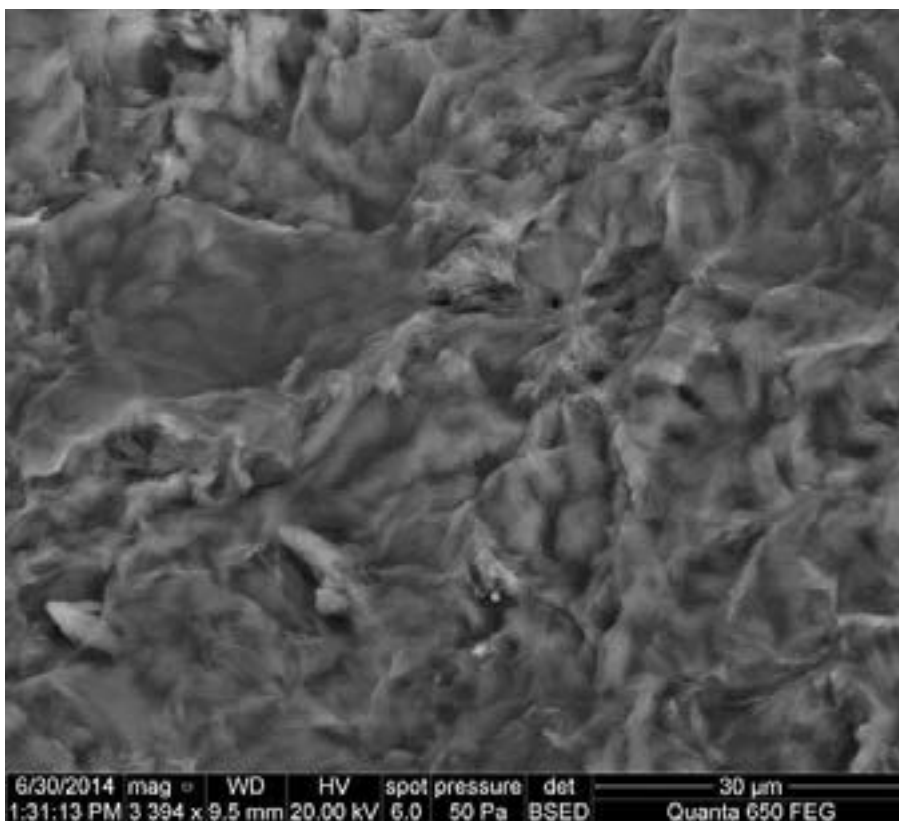


Figure 22:

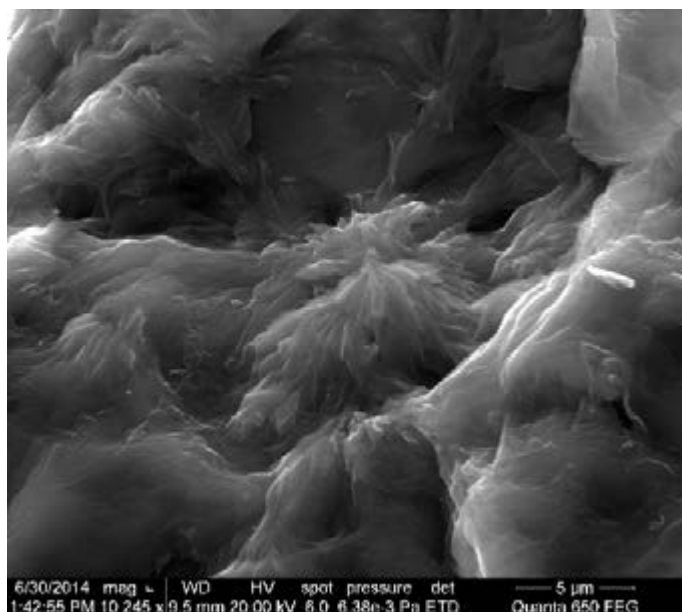


Figure 23:

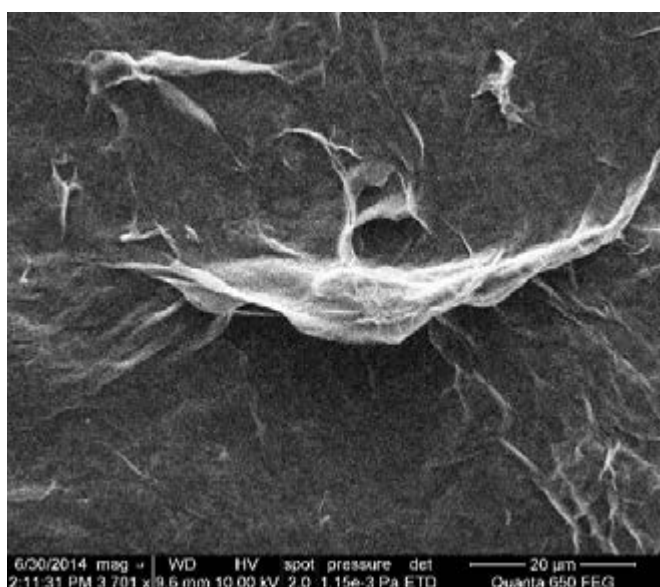


Figure 24:

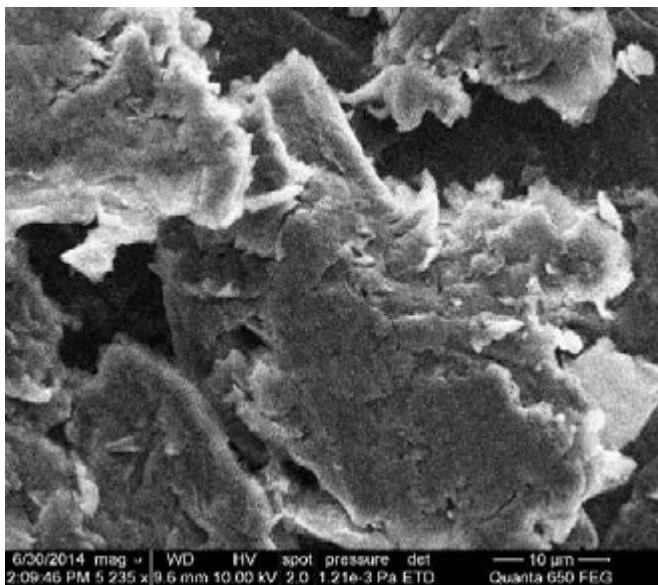


Figure 25:

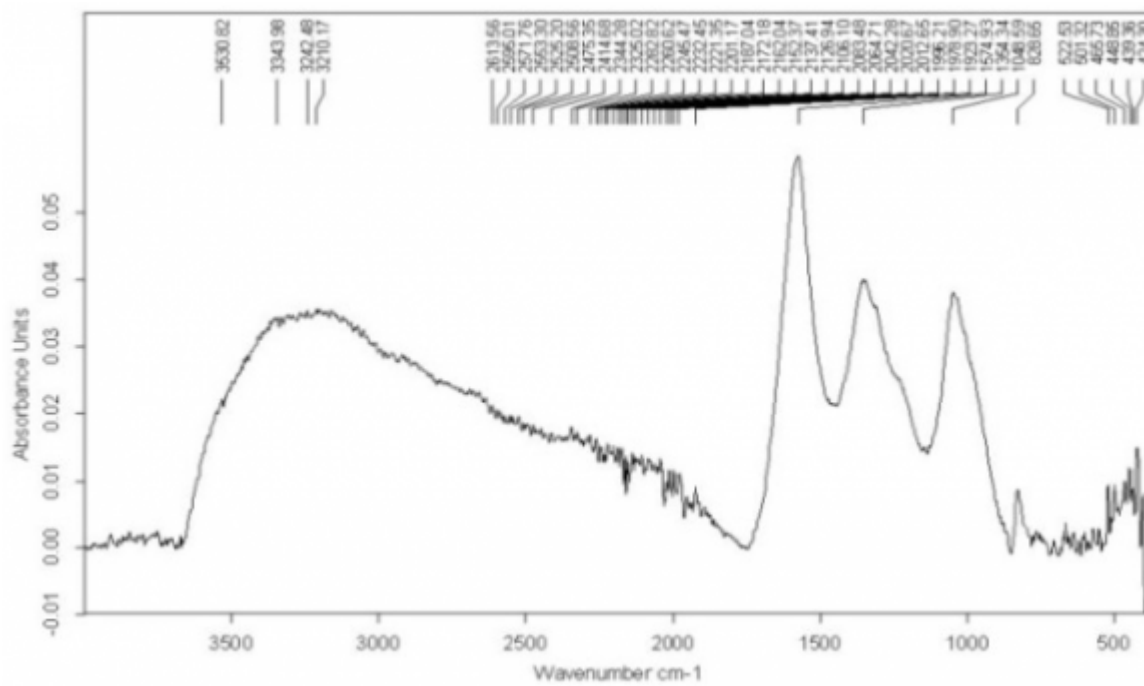


Figure 26:

## 9 CONCLUSION

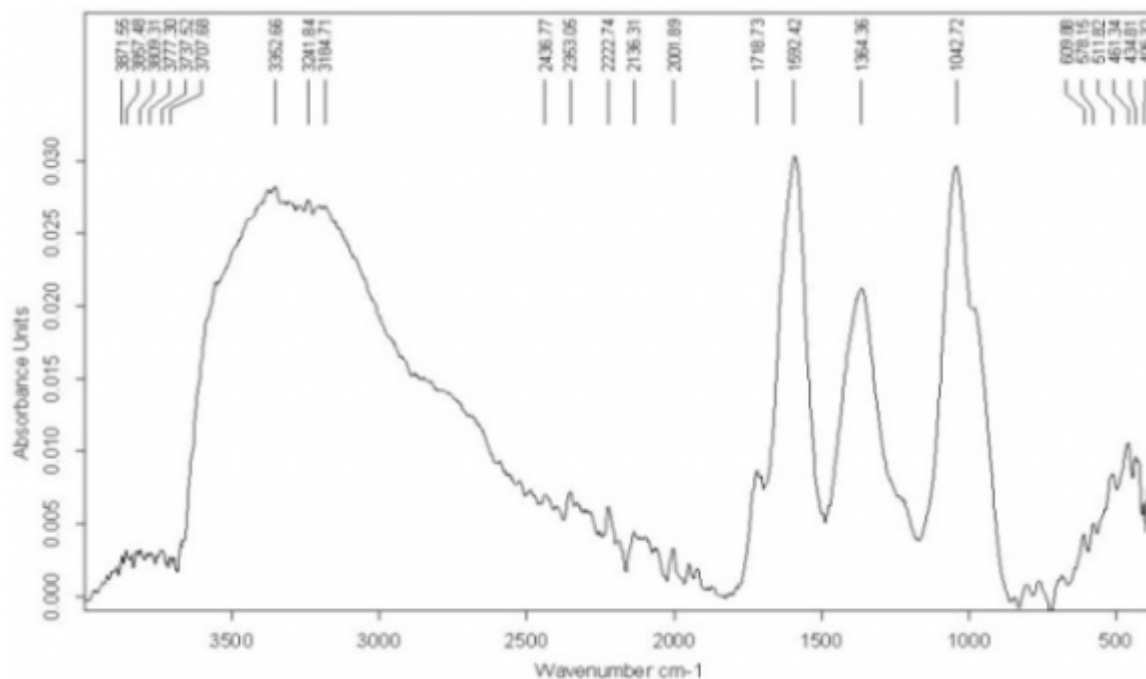


Figure 27:

2

Sample No.	Interval No.	Temperature range (°C)	Weight loss (%)
GO foils	1	25.0 -142.4	11.0
	2	142.4 -213.5	8.8
	3 4	213.5 -222.3 222.3 -368.8	43.6 2.8
	5	368.8 -473.0	18.1
	6	473.0 -600.0	6.1
	GO-C 60 foils	1	25.0 -87.1
2		87.1 -153.0	8.2
3 4		153.0 -197.0 197.0 -205.0	8.0 51.1
5		205.0 -281.3	10.8
6		281.3 -490.9	18.0

Figure 28: Table 2 :

**3**

Sample No.	Thermal process No.	Temperature range (°C)	$\hat{I}^{\circ}H$ (kJ/kg) *	H (mW)	f1	$\hat{I}^{\circ}H$ (kj/kg)
GO foils	1	25.0 -154.1	874.6	15.8		
	2	190.9 -241.1	-508.4	107.4		-910.6
	3	356.5 -492.1	-1277.1	31.0		
GO-C 60 foils	1	42.0 -124.2	141.7	6.4		
	2	182.6 -221.5	-308.7	71.1		-1204.1
	3	319.7 -481.6	-1037.1	28.1		

[Note:  $\hat{I}^{\circ}H$  = thermal effect of the process based on the DSC curves ( $\hat{I}^{\circ}H > 0$  endothermic process,  $\hat{I}^{\circ}H < 0$  exothermic process) Global Journal of Researches in Engineering ( ) Volume XIV Issue I Version I Year 2014]

Figure 29: Table 3 :

**4**

Sample No.	Interval No.	Temperature range (°C)	Weight loss (%)
GO-C 60 -cel.	1	25.0 -42.4	0.3
	2	42.4 -123.9	6.9
	3 4	123.9 -168.9 168.9 -347.8	11.9 18.5
	5	347.8 -474.3	36.4
	6	474.3 -600.0	6.8
	GO -cel.	1	25.0 -57.3
2		57.3 -120.8	10.1
3		120.8 -144.6	3.0
4		144.6 -180.6	13.2
5		180.6 -396.5	20.6
6		396.5 -522.6	48.3
7		522.6 -545.0	2.5
cellulose	1	25.0 -62.9	8.5
	2	62.9 -124.9	55.6
	3	124.9 -265.8	3.3
	4	265.8 -333.4	15.8
	5	333.4 -600.0	10.5

Figure 30: Table 4 :

## 9 CONCLUSION

5

Sample No.	Thermal process No.	Temperature range (°C)	$\hat{I}^*H$ (kJ/kg)*	H fl (mW)	$\hat{I}^*H$ (kJ/kg)
GO-C 60 -cel.	1	31.6 -115.3	159.9	5.7	
	2	115.3 -187.2	-251.1	18.7	-3470.2
	3	319.8 -531.0	-3379.0	59.2	
GO -cel.	1	25.0 -133.1	757.5	17.7	
	2	133.1 -208.1	-581.2	41.7	-5085.1
	3	341.54 -557.2	-5261.4	76.8	
cellulose	1	25.0 -154.0	3053.7	86.2	
	2	247.9 -344.8	-211.3	12.2	+2805.7
	3	372.0 -414.6	-36.7	2.3	

\* $\hat{I}^*H$  = thermal effect of the process based on DSC curves  
( $\hat{I}^*H > 0$ ?endothermic process,  $\hat{I}^*H < 0$ ?exothermic process)

Figure 31: Table 5 :

6

Sample No.	Interval No.	Temperature range (°C)	Weight loss(%)
BG	1	25.0 -114.4	5.5
	2	114.4 -278.1	8.6
	3 4	278.1 -330.3 330.3 -412.7	52.2 17.0
	5	412.7 -462.4	14.8
	6	462.4 -475.9	14.8
	GO-BG	1	25.0 -149.4
2		149.4 -225.5	12.3
3 4		225.5 -292.3 292.3 -337.9	4.7 26.7
5		337.9 -438.4	15.7
6		438.4 -529.8	30.7
GO-BGH +		1	25.0 -124.2
	2	124.2 -204.2	4.2
	3 4	204.2 -230.8 230.8 -321.6	10.9 22.5
	5	321.6 -480.9	25.9
	6	480.9 -550.2	26.9

[Note: X-the indicated intersections of tangents to the respective bends of the TGA curve]

Figure 32: Table 6 :

7

Sample No.	Thermal processNo.	Temperature range (°C)	$\hat{I}^{\circ}H$ (kJ/kg) *	H fl (mW)	$\hat{I}^{\circ}H$ (kJ/kg)
BG	1 2	25.0 -153.9 257.5 -528.4	805.9 -4392.5	21.3 81.0	-3586.6
	1	25.0 -157.0	825.3	16.9	
GO-BG	2 3	157.0 -228.8 311.0 -356.5	-147.1 -36.3	8.9 6.2	-2734.9
	4	383.3 -539.3	-3376.8	66.4	
GO-BGH	1	25.0 -145.9	685.2	16.7	
	2	197.2 -250.0	-313.5	38.2	-2084.7
+	3	425.4 -589.3	-2456.4	46.2	

Figure 33: Table 7 :



272 [ Chemical Society Reviews] , *Chemical Society Reviews* 19 p. .

273 [ J. Phys. Chem. C] , *J. Phys. Chem. C* 116 (43) p. .

274 [ Sensors (Basel)] , *Sensors (Basel)* 13 (12) p. .

275 [Hu et al. ()] ‘A Facile Route for the Large Scale Fabrication of Graphene Oxide Papers and Their Mechanical  
276 Enhancement by Cross-linking with Glutaraldehyde’. N Hu , L Meng , R Gao , Y Wang , J Chai , Z Yang ,  
277 E.S-W Kong , Y Zhang . *Nano-Micro Letters* 2011. 3 (4) p. .

278 [Chabot et al. ()] ‘A review of graphene and graphene oxide sponge: materialsynthesis is and applications to  
279 energy and the environment’. V Chabot , D Higgins , A Yu , X Xiao , Z Chen , J Zhang . *Energy Environ.*  
280 *Sci* 2014. 7 p. .

281 [Faye ()] ‘Adatom Adsorption on Graphene: A First-Principle Study’. O Faye . *The African Review of Physics*  
282 2012. 7 p. 315.

283 [Neto ()] ‘Adatoms in Graphene’. A H C Neto . *Solid State Communications* 2009. 149 p. .

284 [Fakhri ()] ‘Adsorption characteristics of graphene oxide as a solid adsorbent for aniline removal from aqueous  
285 solutions: Kinetics, thermodynamics and mechanism studies’. A Fakhri . *Journal of Saudi Chemical Society*  
286 2013.

287 [Shen et al. ()] ‘Bio medical Applications of Graphene’. H Shen , L Zhang , M Liu , Z Zhang . *The nanostics*,  
288 2012. 2 p. .

289 [Navalon et al. ()] ‘Carbo catalysis by Graphene-Based Materials’. S Navalon , A Dhakshinamoorthy , M Alvaro  
290 , H Garcia . *Chem. Rev* 2014. 114 (12) p. .

291 [Su and Loh ()] ‘Carbo catalysts: Graphene Oxide and Its Derivatives’. Ch Su , K P Loh . *Acc. Chem. Res* 2013.  
292 46 (10) p. .

293 [Li and Ragauskas (ed.) ()] *Cellulose Nano Whiskers as a Reinforcing Filler in Polyurethanes. Advances in*  
294 *Diverse Industrial Applications of Nano composites*, Y Li , A J Ragauskas . Dr.BoreddyReddy (ed.) 2011.

295 [Peng et al. ()] ‘Chemistry and Applications of Nano crystalline Cellulose and its Derivatives: A nano technology  
296 Perspective’. B L Peng , N Dhar , H L Liu , K C Tam . *The Canadian Journal of Chemical Engineering* 2011.  
297 p. 9999.

298 [Liao et al. ()] ‘Cytotoxicity of Graphene Oxide and Graphene in Human Erythrocytes and Skin Fibroblasts’.  
299 K-H Liao , Y-S Lin , Ch W Macosko , . L Haynes Ch . *ACS Appl. Mater. Interfaces* 2011. 3 p. .

300 [effect of concentration of graphene nano platelets on mechanical and electrical properties of reduced graphene oxide papers] Global  
301 ‘effect of concentration of graphene nano platelets on mechanical and electrical properties of reduced graphene  
302 oxide papers’. *Global Journal of Researches in Engineering* 50 p. . (Carbon)

303 [Krishnan et al. ()] ‘Energetic Graphene oxide: Challenges and opportunities’. D Krishnan , F Kim , J Luo , R  
304 Cruz-Silva , L J Cote , H Jang , J Huang . *Nano today* 2012. 7 p. .

305 [Zhang et al. ()] ‘Functionalization of graphene sheets through fullerene attachment’. Y Zhang , L Ren , S Wang  
306 , A Marathe , J Chaudhuri , G Li . *Journal of Materials Chemistry* 2011. 21 p. 5386.

307 [Yoo et al. ()] ‘Graphene and graphene oxide and their uses in barrier polymers’. B M Yoo , H J Shin , H W  
308 Yoon , H B Park . *Journal of Polymer Science: Polymer Physics* 2013.

309 [Kyzas et al. ()] ‘Graphene oxide and its application as an adsorbent for waste water treatment’. G Z Kyzas , E  
310 A Deliyanni , K A Matis . *J. Chem. Technol. Bio technol* 2014. 89 p. .

311 [Makharza et al. ()] ‘Graphene oxide-based drug delivery vehicles: functionalization, characterization, and  
312 cytotoxicity evaluation’. S Makharza , G Cirillo , A Bachmatiuk , I Ibrahim , N Ioannides , B Trzebicka , S  
313 Hampel , M H Rummeli . *Journal of Nano part Res* 2013. 15 p. 2099.

314 [Wang et al. ()] ‘Green and easy synthesis of biocompatible graphene for use as an anti-coagulant’. Y Wang , P  
315 Zhang , Ch F Lie , Y Zhan , Y F Li , Ch Z Huang . *The Royal Society of Chemistry* 2012. 2 p. .

316 [Trzaskowski et al. ()] ‘Impact of Local Curvature and Structural Defects on Graphene-C60 Fullerene Fusion  
317 Reaction. B Barriers’. B Trzaskowski , L Adamowicz , W Beck , K Muralidharan . *J. Phys. Chem* 2013.  
318 19669-19671.

319 [Klouda ()] *Interkalární sloučeniny grafitu. (Intercalation compounds of graphite)Dissertation, V?CHT Praha*,  
320 K Klouda . 1985. (available in the technical library in Prague 6 -Dejvice)

321 [Ioelovich ()] ‘Optimal Conditions for Isolation of Nano crystal line Cellulose Particles’. M Ioelovich . *Nano*  
322 *science and Nanotechnology* 2012. 2 (2) p. .

323 [Bondeson et al. ()] ‘Optimization of the isolation of nanocrystals from microcrystalline cellulose by acid hydrolysis’.  
324 D Bondeson , A Mathew , K Oksman . *Cellulose* 2006. 13 p. .

325 [Troshin and Lyubovskaya ()] ‘Organic chemistry of fullerenes: the major reactions, types of fullerene derivatives  
326 and prospects for their practical use’. P A Troshin , R N Lyubovskaya . *Russian Chemical Reviews* 2008. 77  
327 (4) p. .

## 9 CONCLUSION

---

- 328 [Rodríguez-González et al. ()] 'Polysaccharide Nano composites Reinforced with Graphene Oxide and Keratin-  
329 Grafted Graphene Oxide'. C Rodríguez-González , A L Martínez-Hernández , V Castano , O V Kharissova ,  
330 R S Ruoff , C Velasco-Santos . *Industrial & Engineering Chemistry Research* 2012. 51 p. .
- 331 [Saeedfar et al. ()] *Potentiometric Urea Biosensor Based on an Immobilised Fullerene-Urease Bio-Conjugate*, K  
332 Saeedfar , L Y Heng , T L Ling , M Rezayi . 2013.
- 333 [Hummers and Offeman ()] 'Preparation of Graphitic Oxide'. W S Hummers , R E Offeman . *J. Am. Chem. Soc*  
334 1958. 80 (6) p. 1339.
- 335 [Zhu et al. ()] *Selectively Expanding Graphene Oxide Paper for Creating Multifunctional Carbon Materials*, J  
336 Zhu , L Zhu , Z Lu , L Gu , S Cao , X Cao . 2012.
- 337 [Peng et al. ()] 'Simultaneous Reduction and Surface Functionalization of Graphene Oxide by Natural Cellulose  
338 with the Assistance of the Ionic Liquid'. H Peng , L Meng , L Niu , Q Lu . *The Journal of Physical Chemistry*  
339 2012. 116 p. .
- 340 [Kabir et al. ()] 'Substantial reduction of Stone-Wales activation barrier in fullerene'. M Kabir , S Mukherjee ,  
341 T Saha-Das Gupta . *Physical Review* 2011.
- 342 [Chen et al. ()] 'Surfaceamorphization and deoxy genation of graphene oxide paper by Ti ion implantation'. J  
343 Chen , G Zhang , B Luo , D Sun , X Yan , Q Ue . *Carbon* 2011. 49 p. .
- 344 [Russo et al. ()] 'Synthesis, Properties and Potential Applications of Porous Graphene: A Review'. P Russo , A  
345 Hu , G Compagnini . *Nano-microletters* 2013. 5 (4) p. .
- 346 [Dreyer et al. ()] *The chemistry of grapheme oxide*, D R Dreyer , S Park , Ch W Bielawski , R S Ruoff . 2010.
- 347 [Chng and Pumera ()] 'The Toxicity of Graphene Oxides, Dependence on the Oxide line Methods'. E L K Chng  
348 , M Pumera . *Chem. Eur. J* 2013. 19.
- 349 [Chovancová and ?turdík ()] *Vliv beta glukánovnaïmunitní systém?lov?ka (Effects of beta glucans in human*  
350 *immunity system)*, A Chovancová , E ?turdík . 2005. Nova Biotechnologica, V-I. p. .